EARLY HETEROGENIC RESPONSE OF RENAL MICROVASCULATURE TO HEMORRHAGIC SHOCK/RESUSCITATION AND THE INFLUENCE OF NF-κB PATHWAY BLOCKADE

Rui Yan,* Matijs van Meurs,*† Eliane R. Popa,* Ranran Li,*‡ Peter J. Zwiers,* Jan G. Zijlstra,† Jill Moser,*† and Grietje Molema*

*Department of Pathology and Medical Biology, Medical Biology Section, University Medical Center Groningen, University of Groningen, Groningen, The Netherlands; †Department of Critical Care, University Medical Center Groningen, University of Groningen, Groningen, The Netherlands; and ‡Department of Critical Care Medicine, Ruijin Hospital, Shanghai Jiao Tong University School of Medicine, Shanghai, China

ABSTRACT—Hemorrhagic shock (HS) is associated with low blood pressure due to excessive loss of circulating blood and causes both macrocirculatory and microcirculatory dysfunction. Fluid resuscitation after HS is used in the clinic to restore tissue perfusion. The persistent microcirculatory damage caused by HS and/or resuscitation can result in multiple organ damage, with the kidney being one of the involved organs. The kidney microvasculature consists of different segments that possess a remarkable heterogeneity in functional properties. The aim of this study was to investigate the inflammatory responses of these different renal microvascular segments, i.e., arterioles, glomeruli, and postcapillary venules, to HS and resuscitation (HS/R) in mice and to explore the effects of intervention with a nuclear factor-kappa B (NF-κB) inhibitor on these responses. We found that HS/R disturbed the balance of the angiopoietin-Tie2 ligand-receptor system, especially in the glomeruli. Furthermore, endothelial adhesion molecules, proinflammatory cytokines, and chemokines were markedly upregulated by HS/R, with the strongest responses occurring in the glomerular and postcapillary venous segments. Blockade of NF-κB signaling during the resuscitation period only slightly inhibited HS/R-induced inflammatory activation, possibly because NF-κB p65 nuclear translocation already occurred during the HS period. In summary, although all three renal microvascular segments were activated upon HS/R, responses of endothelial cells in glomeruli and postcapillary venules to HS/R, as well as to NF-κB inhibition were stronger than those in arterioles. NF-κB inhibition during the resuscitation phase does not effectively counteract NF-κB p65 nuclear translocation initiating inflammatory gene transcription.

KEYWORDS—Endothelium, hemorrhagic shock/resuscitation, inflammatory response, microvascular segments, NF-κB inhibition, renal microvasculature

INTRODUCTION

Hemorrhagic shock (HS) is a pathophysiological condition that is caused by excessive loss of blood and a dramatic drop in blood pressure. HS is characterized by reduced tissue blood perfusion that is accompanied by inadequate delivery of oxygen and nutrients that are necessary for cellular function. Fluid resuscitation after HS to restore tissue perfusion is an important intervention method in the clinic (1). Despite treatment advances, HS patients and survivors of HS and resuscitation (HS/R) often develop multiple organ dysfunction syndrome (MODS) (2). Among the failing organs, the kidney is one of the most vulnerable, and acute kidney injury (AKI) is strongly associated with morbidity and mortality in critically injured patients (3). We propose that early intervention to halt AKI development during the resuscitation period will protect the kidney from extensive damage.

Vascular endothelium lines the inner walls of the entire vascular system and displays a remarkable heterogeneity in functional properties, in health and disease (4). This microvascular heterogeneity does not only exist in the different microvascular beds in different organs, but also in different microvascular segments within one organ (5). Endothelial cells (ECs) in different renal microvascular compartments demonstrate unique structural and functional properties to support kidney function and homeostasis (6).

The existence of heterogeneity in endothelial responsiveness to inflammatory stimuli is nowadays well accepted (7). In one of our previous studies on systemic inflammation in mice induced by HS and resuscitation, we showed that E-selectin protein became highly expressed in glomeruli, whereas it was much less expressed in the other renal microvascular segments. In contrast, VCAM-1 protein was highly expressed in extra-glomerular segments and scarcely present in glomerular endothelium (8). This molecular heterogeneity in responsiveness of renal microvascular segments to inflammatory stress likely finds its origin in variation in transcriptional and posttranscriptional control between endothelial cells in different microvascular segments (9). Studying renal microvascular

compartment phenotypes plays an important role in understanding the molecular basis for basic phenotypic heterogeneity, as well as for the heterogeneity in pathophysiological responses during kidney injury.

Nuclear factor-kappa B (NF-κB) is a transcription factor that is actively involved in the regulation of the expression of endothelial inflammatory response genes and plays a pivotal role in the onset of an inflammatory response (10, 11). Increasing evidence at organ level shows that inhibition of NF-κB activation before, or during resuscitation can reduce kidney, liver, and lung injury and dysfunction induced by HS (12–14). In addition, we previously found that blockade of NF-κB signaling ameliorates microvascular proinflammatory responses in the kidney of HS/R mice (15).

Here we hypothesized that the responses of the endothelium of different renal microvascular segments, and the effects of therapeutic intervention on these segments, vary in responses to HS/R. To investigate this hypothesis, we isolated renal microvascular beds by laser microdissection, i.e., arterioles, glomeruli, and postcapillary venules, and subjected them to gene expression analysis. Laser microdissection (LMD) separates the microvascular compartments from tissue sections without affecting RNA integrity (16). We explored the gene expression levels of vascular stability related molecules, endothelial proinflammatory molecules, and intracellular signaling molecules in response to HS/R in the three microvascular segments in mouse kidney. We furthermore examined the consequences of drug intervention with NF-κB inhibitor BAY11-7082 during resuscitation on the inflammatory response of the renal microvascular endothelium. Immunohistochemical staining was performed to validate the findings for the adhesion molecules at protein level while NF-κB nuclear translocation during the HS and resuscitation phases, and the effect on this translocation by BAY11-7082 treatment was analyzed by immunofluorescence (IF) staining of tissue sections.

MATERIALS AND METHODS

Mice and HS/resuscitation model

Male C57Bl6 mice (8–12 weeks old) from Harlan (Horst, The Netherlands) were housed in temperature-controlled chambers (24°C) with a 12-h light/dark cycle in a specific pathogen-free facility, and received chow and water *ad libitum*. All experiments were performed in compliance with the regulations of the animal ethics committee of the University of Groningen. The experimental setup used in this study was described elsewhere (15).

Briefly, after anesthetizing with isoflurane (inspiratory, 1.4%), N_2O (66%), and O_2 (33%) (8), HS was achieved by blood withdrawal from the left femoral artery, until the mean arterial pressure (MAP) was reached to 30 mmHg. After 90 min of HS, mice were resuscitated with 4% human albumin in saline (AL; Sanquin, Amsterdam, The Netherlands) using 2 times the volume of withdrawn blood. I kappa B kinase (IKK) inhibitor BAY11-7082 (Enzo life Sciences, Lausen, Switzerland) was dissolved in dimethyl sulfoxide (DMSO) to obtain a 40 mg/mL stock concentration. For resuscitation, 10 μL of this stock solution resp. DMSO as vehicle was added per mouse to 4% human albumin. The volume of resuscitation fluid needed per mouse was determined during execution of the experiment and ranged between 1 and 2 mL. The final DMSO concentration hence ranged between 1% and 0.5% (v/v) in the resuscitation fluid. After volume resuscitation with BAY11-7082 at 400 μg per mouse and vehicle, mice were allowed to recover

for 1 h and were subsequently sacrificed. Figure 1A illustrates the study experimental setup.

Groups included control mice (left untreated and terminated at the start of the experiment), HS mice (sacrificed at the end of the 90-min HS period without fluid resuscitation), HS/R mice (HS resuscitated with 4% AL containing vehicle DMSO), and HS/R/BAY mice (HS resuscitated with 4% AL containing BAY11-7082). Mice in the HS/R and HS/R/BAY groups were sacrificed 1 h after resuscitation. During termination, mice were anesthetized with isoflurane, blood was drawn via cardiac puncture, and the organs were harvested, snap-frozen in liquid nitrogen, and stored at −80°C until analysis. Each group consisted of eight mice (15), of which five mice were randomly chosen for further laser microdissection before mRNA analysis and eight mice for immunohistochemical assessment. As in previous studies on HS/resuscitation the highest proinflammatory activation was observed at 1 h after resuscitation (8, 15), we chose this time point to analyze in the present study.

Laser microdissection of the renal microvascular segments

Nine-micrometer thick cryosections from snap-frozen mouse kidneys (n = 5/group) were fixed, stained, and after washing and air-drying, sections were used for laser microdissection (LMD, Leica LMD7000; Leica Microsystems, Germany) to collect arteriolar vascular segments (minimum area $5 \times 10^5 \, \mu m^2$), glomeruli (minimum area $1 \times 10^6 \, \mu m^2$), and venules (minimum area $1 \times 10^6 \, \mu m^2$). Laser microdissected samples were collected in 0.5 mL AdhesiveCap tubes (ZEISS, Göttingen, Germany) and stored at −80°C for further analysis. Leftover cryosections from LMD was collected in 350 μL RLT buffer (Qiagen) as post-LMD samples and stored at −80°C until further analysis.

Gene expression analysis by reverse transcription-quantitative PCR

Total RNA from whole kidney sections was isolated using the RNeasy Mini plus Kit (Qiagen) and total RNA from LMD materials was isolated with RNeasy Micro Plus Kit (Qiagen) according to the manufacturer's instructions. The integrity of RNA from whole kidney sections and post-LMD samples was determined by gel electrophoresis. Concentration and purity of RNA from whole kidney section isolates was assessed by a NanoDrop ND-1000 UV-Vis spectrophotometer (NanoDrop Technologies, Rockland, Del). For cDNA synthesis, total RNA was reversed transcribed using Superscript III Reverse Transcriptase (Invitrogen, Breda, The Netherlands) as described previously (17).

Gene expression analysis was performed using Taqman custom-designed, low-density array cards (Applied Biosystems, Nieuwerkerk aan den IJssel, The Netherlands). The low-density array cards contained assays for 24 genes that were chosen based on their roles in vascular permeability/integrity, inflammation, and basic endothelial cell behavior. GAPDH was chosen as housekeeping gene and 18S rRNA was a mandatory control provided by the manufacturer.

PCR amplification of the low-density array cards was performed in a ViiA 7 real-time PCR System (Applied Biosystems) according to the manufacturer's protocol. mRNA values were obtained by the comparative threshold cycle (CT) values method. For each sample, CT values of duplicate reactions were averaged. The error, which is equal to the average of the two duplicate CT values minus the smallest value of the two, was used to evaluate the variation in technical replicates, as a means to determine the accuracy of measurement of the CT value. A sample with a CT error above 0.5 was considered an unacceptable technical replicate. Both unacceptable samples and undetermined samples [no CT value was obtained in reverse transcription-quantitative PCR (RT-qPCR) reaction] were eliminated from further data analysis. In case all samples in a group yielded unacceptable/undetermined values, we annotated them as ND (not detectable). In all other instances, each accurate replicate is reported.

Gene expression was normalized to the expression of the housekeeping gene GAPDH, resulting in the ΔCT value. The pan-endothelial marker VE-cadherin was used as reference gene to correct for the content of endothelium in LMD samples in case of analyzing endothelial-restricted genes. The mRNA levels relative to GAPDH, or VE-cadherin, were calculated by $2^{-\Delta CT}$.

Immunohistochemical detection of endothelial cell adhesion molecules in mouse kidney

The expression and localization of E-selectin, VCAM-1, and ICAM-1 proteins in mouse kidney were determined by immunohistochemistry (IHC).
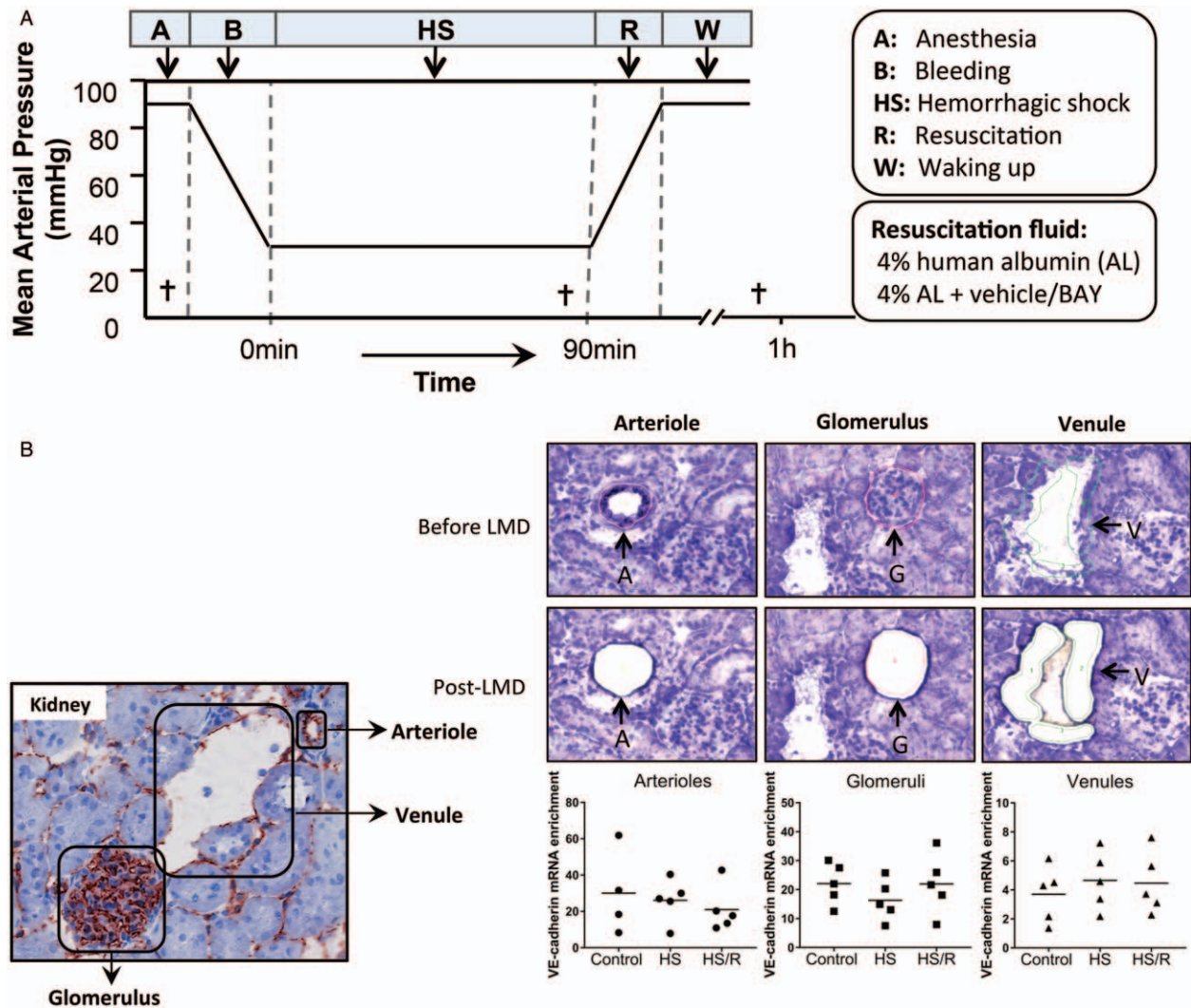
FIG. 1. **Schematic representation of the experimental setup used in this study.** (A) Mouse model for hemorrhagic shock and resuscitation. Hemorrhage was achieved by blood withdrawal, as described in "Materials and Methods." Mice were terminated (†) at the start of the experiment (control), at the end of the 90-min period of hemorrhagic shock (HS), or at 1 h after resuscitation in the presence of vehicle or NF-κB inhibitor BAY11-7082 (HS/R vs. HS/R/BAY) (15). (B) Laser microdissection of the three renal microvascular segments to study segment-specific responses, and endothelial enrichment of VE-cadherin in these segments. (Top) Annotation of the three renal microvascular compartments used in this study as identified by immunohistochemical (IHC) staining of the pan-endothelial cell marker VE-cadherin. (Bottom) Photomicrographs of hematoxylin-stained mouse kidney showing arteriole, glomerulus, and venule before and after laser microdissection (LMD). The thin colored lines indicate structures to be microdissected. VE-cadherin mRNA enrichment in the segments was determined by RT-qPCR using GAPDH as housekeeping gene as described in "Materials and Methods." Values represent enrichment in VE-cadherin mRNA levels in the vascular segments as compared with its mRNA levels in whole kidney sections from the same mouse. Individual values and means are shown for each group. A, arteriole; G, glomerulus; V, venule. Original magnification: 200×.

Five-micrometer acetone-fixed kidney cryosections from snap-frozen mouse kidneys were incubated with Peroxidase Block (EnVision + System-HRP (AEC); DAKO, Carpentaria, Calif) for 10 min to block endogenous peroxidase. For specific protein detection, sections were incubated with primary rat anti-mouse antibodies against E-selectin (MES-1; hybridoma supernatant, 1:10, kindly provided by Dr Derek Brown, UCB Celltech, Belgium), VCAM-1 (1:10, clone MIK-1.9; ATCC, Manassas, Va), ICAM-1 (5 μg/mL; Southern Biotech, Birmingham, AL), and CD31 (1:100, cat. no. #550274; BD Pharmingen, San Diego, Calif, for endothelial all detection, data not shown) all diluted in 5% fetal calf serum (FCS; Sigma-Aldrich, St. Louis, Mo) in PBS for 1 h at room temperature (RT). After washing, sections were incubated with rabbit anti-rat IgG antibody (mouse adsorbed; Vector Laboratories, Burlingame, Calif) diluted 1:300 in 5% FCS/2% normal mouse serum (Sanquin, Amsterdam, The Netherlands) in PBS for 45 min at RT. After washing, sections were incubated with anti-rabbit labeled polymer HRP antibody from the EnVision kit for 30 min at RT. To visualize peroxidase activity, 3-amino-9-

ethylcarbazole (AEC) from the EnVision kit was used and sections were subsequently counterstained with Mayer's hematoxylin (Merck, Darmstadt, Germany).

Semiquantitative analysis of immunohistochemical staining of renal microvascular segments

Slides were scanned using the NanoZoomer 2.0-HT (Hamamatsu, K.K., Japan) to acquire whole slide digital images. Images were viewed and analyzed using ImageScope analysis software (version 12.2; Aperio Technologies, Inc.). The positive pixel count algorithm (version 9.1) of the ImageScope analysis software was applied to quantify the IHC staining. Briefly, regions of interest (ROI) were drawn around the perimeter of kidney sections using the free-hand pen tool, excluding damaged areas and the renal medulla. The percentage of positive (stained) pixels was calculated relative to the number of total (positive and negative) pixels in a ROI. To quantify

staining in selected microvascular segments, ROI were drawn around the respective segments, and the percentage of positive pixels was determined as described above. The quantitation was done for E-selectin, VCAM-1, and ICAM-1 in whole kidney sections, arterioles, glomeruli, and venules (8 mice/group).

Immunofluorescence double staining for NF-κB p65 and CD31 in mouse kidneys

Immunofluorescence double staining was performed on 5-μm cryosections from snap-frozen mouse kidneys. After acetone fixation, sections were incubated with primary rabbit anti-p65 antibody (1:200, #D14E12; Cell Signaling Technology, Leiden, The Netherlands) and rat anti-CD31 antibody (1:200, #550274; BD Pharmingen, San Diego, Calif) in PBS containing 5% FCS for 1 h at RT. After washing, sections were incubated with Alexa Fluor555-conjugated donkey anti-rabbit secondary antibody (A-31572; Thermo Fisher, Waltham, Mass) to detect p65, and goat anti-rat Alexa Fluor488 secondary antibody to detect CD31 (A-11006; Thermo Fisher) in PBS with 5% FCS plus 2% normal mouse serum (Sanquin) for 45 min at RT. After washing, sections were incubated with 0.1% Sudan Black B (Sigma-Aldrich) in 70% ethanol for 30 min at RT. Thereafter, sections were washed 3 times and mounted in Aqua/Polymount medium containing DAPI (Polysciences, Warrington, Pa). Fluorescence images were taken using a Leica DM4000B fluorescence microscope (Leica Microsystems Ltd., Germany) with Leica LAS V4.5 image software. All images were taken with equal exposure times.

Statistical analysis

Statistical significance of differences was analyzed by a two-tailed unpaired Student's t test, assuming equal variances to compare two replicate means. To compare multiple replicate means, a one-way analysis of variance (ANOVA) followed by Bonferroni *post hoc* analysis was used. All statistical analyses were performed using GraphPad Prism Software v.7.03 (GraphPad Prism Software Inc., San Diego, Calif). Differences were considered to be significant when $P < 0.05$.

RESULTS

Endothelial enrichment in microvascular endothelial segments laser microdissected from mouse kidney

To investigate microvascular heterogeneity in healthy (control) mouse kidney and to reveal the responses of different renal microvascular segments to HS/resuscitation (HS/R) and therapeutic intervention, we laser microdissected arterioles, glomeruli, and venules, before gene expression analysis (Fig. 1B). Enrichment of mRNA of the pan-endothelial gene VE-cadherin (Fig. 1B) was observed in all segments. Dissected arterioles and glomeruli showed around 20-fold enrichment of VE-cadherin mRNA compared with whole kidney sections from the same mouse. The enrichment of VE-cadherin in venules was approximately 4-fold compared with whole kidney sections (Fig. 1B). In addition, VE-cadherin enrichment in vascular segments was similar in samples obtained from control mice, HS mice, and HS/R mice (Fig. 1B).

Expression levels of vascular stability related molecules in renal microvascular segments in control conditions, and effects of HS and HS/R

To study the effects of the HS period and of HS combined with subsequent resuscitation on renal microvascular responses, mRNA levels of inflammatory genes were determined by RT-qPCR in laser microdissected microvascular segments. For vascular stability related genes, a heterogenic basal expression pattern was observed in microvascular segments of control kidneys (Fig. 2; Supplementary Fig. S1A,

http://links.lww.com/SHK/A710). Although Tie2 was expressed in all segments to a similar extent, its ligands Ang-1 and Ang-2 were mainly detectable in the postcapillary venules and glomeruli. VEGF and its receptor VEGFR2 showed highest expression in glomeruli and a 2- to 3-fold lower expression in arterioles and postcapillary venules (Fig. 2; Supplementary Fig. S1A, http://links.lww.com/SHK/A710). In renal arterioles of control kidneys, VEGF mRNA was hardly detectable, whereas VEGFR2 was more than 5-fold lower than in postcapillary venules and 20-fold lower than in glomeruli. One hour after resuscitation, Tie2 mRNA levels were significantly reduced in arterioles and glomeruli compared with control mice, whereas Ang-2 was enhanced in glomeruli (an effect not visible when analyzing whole kidney sections, see Supplementary Fig. S2, http://links.lww.com/SHK/A710). Downregulation of VEGFR2 expression was prominently observed in glomeruli after 90 min of HS, which even further decreased during the resuscitation phase, whereas its ligand VEGF was not affected in a major way in any of the segments (Fig. 2). In summary, the expression levels of vascular stability related molecules Ang-1, Ang-2, VEGF, and VEGFR2 differed between arterioles, glomeruli, and venules in control kidney, whereas Tie2 was constitutively expressed to the same extent in all microvessels. In conditions of HS and resuscitation, all microvascular beds showed reduced Tie2 expression, whereas glomerular endothelial cells most pronouncedly upregulated Ang-2 and downregulated VEGFR2 expression.

Renal microvascular segments restricted expression of endothelial proinflammatory molecules and their regulation during HS and HS/R

We previously reported that HS/R led to microvascular inflammatory activation in the kidneys (15). To further investigate whether the activation is similarly or differentially regulated in the different renal microvascular beds, mRNA expression of endothelial adhesion molecules and proinflammatory cytokines was analyzed in the three microvascular segments. In healthy mice, expression of P-selectin and E-selectin was virtually absent in all three microvascular beds. VCAM-1 and ICAM-1, on the contrary, could be measured in all microvascular beds with the highest mRNA expression levels in the venules and the lowest in glomeruli. Endomucin, recently identified to have an anti-leukocyte adhesion function (18), was detectable in glomeruli and venules, yet absent in arterioles (Fig. 3A; Supplementary Fig. S1A, http://links.lww.com/SHK/A710). Furthermore, in control conditions the proinflammatory cytokines IL-1β, IL-6, the chemokine GRO1, a murine IL-8 homologue, and MCP-1 were either undetectable or expressed to a minor extent in the three microvascular compartments (Fig. 3B; Supplementary Fig. S1A, http://links.lww.com/SHK/A710). HS alone and HS/R significantly induced P-selectin and E-selectin mRNA levels in glomeruli and venules (Fig. 3A). Moreover, VCAM-1 and ICAM-1 expression already became strongly upregulated in glomeruli and venules within the HS period, and further increased during resuscitation. Endomucin was most distinctly reduced in glomeruli after HS/R (Fig. 3A). During HS, expression of
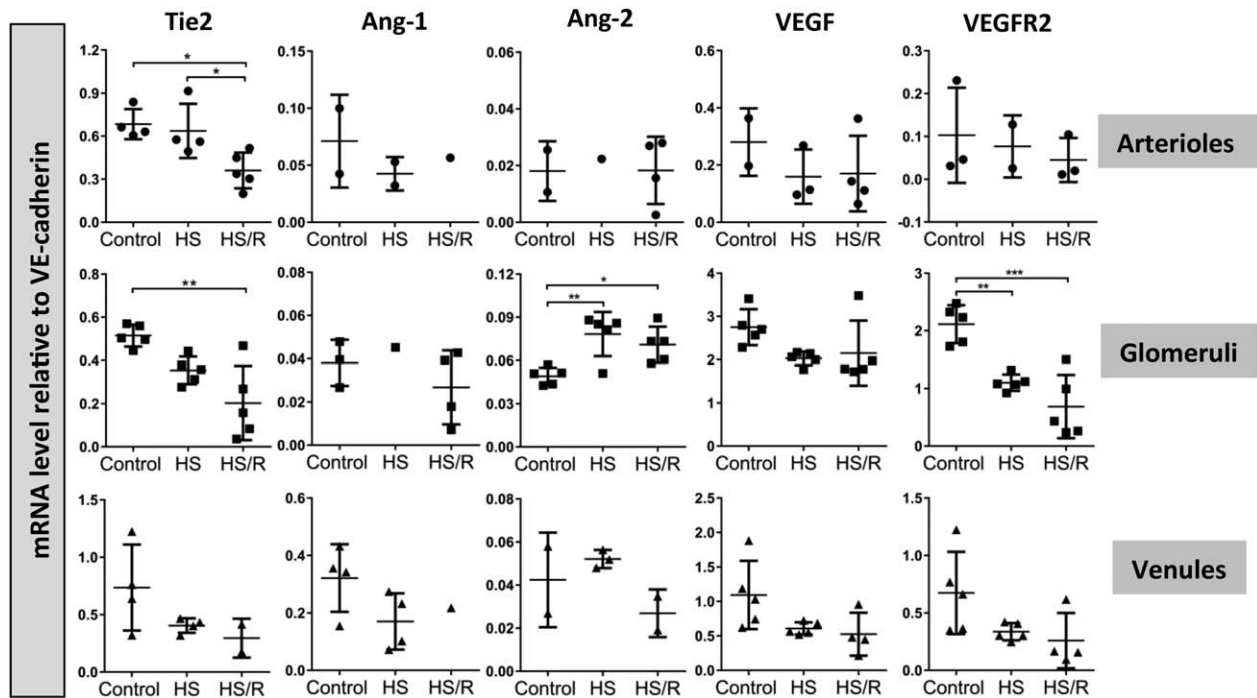
Fig. 2. **Expression levels of vascular stability related molecules in renal microvascular compartments in control conditions, and in HS and HS/R.** Arterioles, glomeruli, and venules were obtained by laser microdissection from snap-frozen mouse kidneys of control group, HS group, and HS/R group. Expression levels of Tie2, Ang-1, Ang-2, VEGF, and VEGFR2 mRNA were determined by RT-qPCR relative to the reference gene VE-cadherin in these microvascular segments. Individual values and mean ± SD are shown for each group. $^{*}P < 0.05$; $^{**}P < 0.01$; $^{***}P < 0.001$. Groups with less than three samples were excluded from the statistical analysis.

proinflammatory cytokines IL-1β, IL-6, and chemokines GRO1, and MCP-1 increased in the three microvascular compartments (Fig. 3B). The resuscitation procedure significantly enhanced IL-1β expression compared with control mice in glomeruli and furthered GRO1 and MCP-1 expression in glomeruli and venules (Fig. 3B).

Overall, these data show that in control mouse kidney the endothelial adhesion molecules P-selectin and E-selectin, proinflammatory cytokines, and chemokines are hardly expressed/absent in arterioles, glomeruli, and venules, whereas adhesion molecules VCAM-1 and ICAM-1 are heterogenically expressed in all three microvascular beds. Endothelial cells in different microvascular segments responded in a segment-specific fashion to HS and HS/R, with glomeruli and postcapillary venules being the responding segments that most prominently upregulated the adhesion molecules, IL-1β, IL-6, GRO1, and MCP-1 while downregulating Endomucin.

Expression of intracellular signaling molecules KLF2, RIG-I, and IRF-1 in renal microvascular compartments in healthy kidney and effects of HS and HS/R

Loss of shear stress rapidly affects shear stress sensor KLF2, which also influences the expression of adhesion molecules E-selectin, VCAM-1 and ICAM-1, and chemokine IL-8 in HUVECs (19). In the presence of TNF-α stimulation, KLF2 can regulate IRF-1 expression in cultured human aortic endothelial cells (20). Our previous study showed that RIG-I

functions as a critical regulator of endothelial activation in response to TNF-α and LPS stimulation (21). We recently found that IRF-1 specifically regulates LPS-mediated VCAM-1 expression in a RIG-I controlled manner (17). In the present study, we therefore determined the response of KLF2, RIG-I, and IRF-1 to HS and HS/R. In control conditions, KLF2 mRNA was more than 7-fold higher expressed in arteriolar and glomerular microvascular segments than in venules. RIG-I expression was approximately 3-fold lower in postcapillary venules than in glomeruli, whereas expression of IRF-1, one of RIG-I's downstream signaling components, was also lowest in postcapillary venules (Fig. 4; Supplementary Fig. S1A, http://links.lww.com/SHK/A710). HS significantly downregulated KLF2 expression, mainly in venules. RIG-I expression did not significantly change during HS and postresuscitation, whereas 1 h after resuscitation IRF-1 expression was markedly upregulated in the glomeruli and venules compared with control conditions (Fig. 4).

Effects of NF-κB inhibitor BAY11-7082 treatment during resuscitation on HS/R-induced endothelial proinflammatory activation in renal microvascular segments

Next, we investigated the effects of therapeutic intervention at the level of NF-κB signaling on endothelial cell activation in the separate renal microvascular beds. Similar to observations in whole kidney analyses (Supplementary Fig. S3, http://links.lww.com/SHK/A710), BAY11-7082 treatment administered
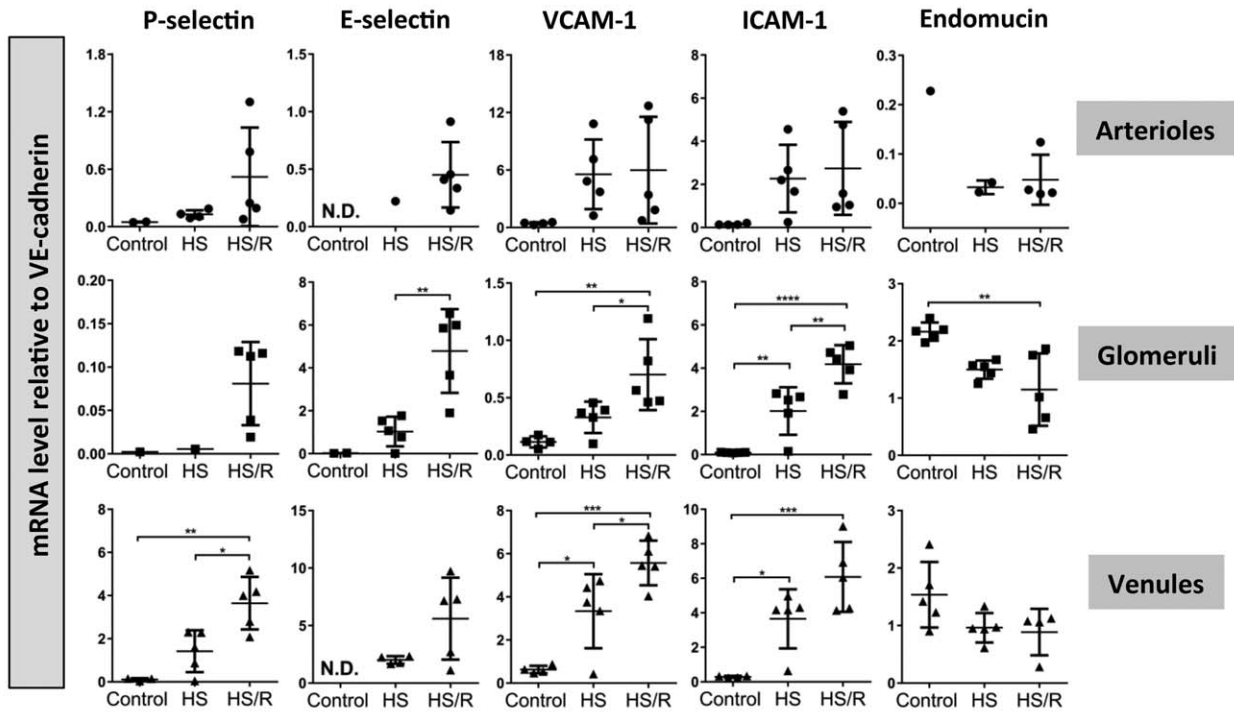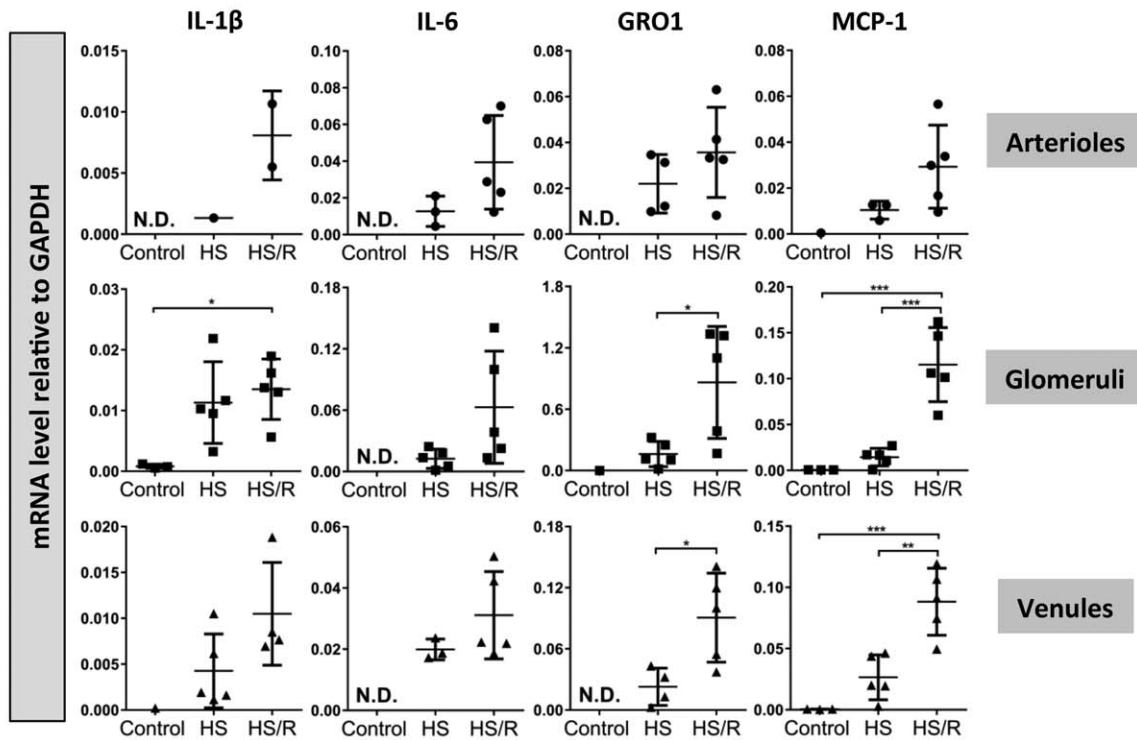
FIG. 3. **Renal microvascular segments restricted expression of endothelial proinflammatory molecules and their regulation during HS and HS/R.** Arterioles, glomeruli, and venules were isolated by laser microdissection from snap-frozen tissues of control mice, HS mice, and HS/R mice. Gene expression levels of (A) adhesion molecules P-selectin, E-selectin, VCAM-1, ICAM-1, and Endomucin, and (B) proinflammatory cytokine IL-1β, IL-6, and chemokines GRO1, MCP-1 were analyzed by RT-qPCR in these microvascular segments. VE-cadherin was used as the reference gene for adhesion molecules, and GAPDH was used as the reference gene for proinflammatory cytokines and chemokines. Individual values and mean ± SD are shown for each group. N.D., not detectable, $^*P < 0.05$; $^{**}P < 0.01$; $^{***}P < 0.001$. Groups with less than three samples were excluded from the statistical analysis.
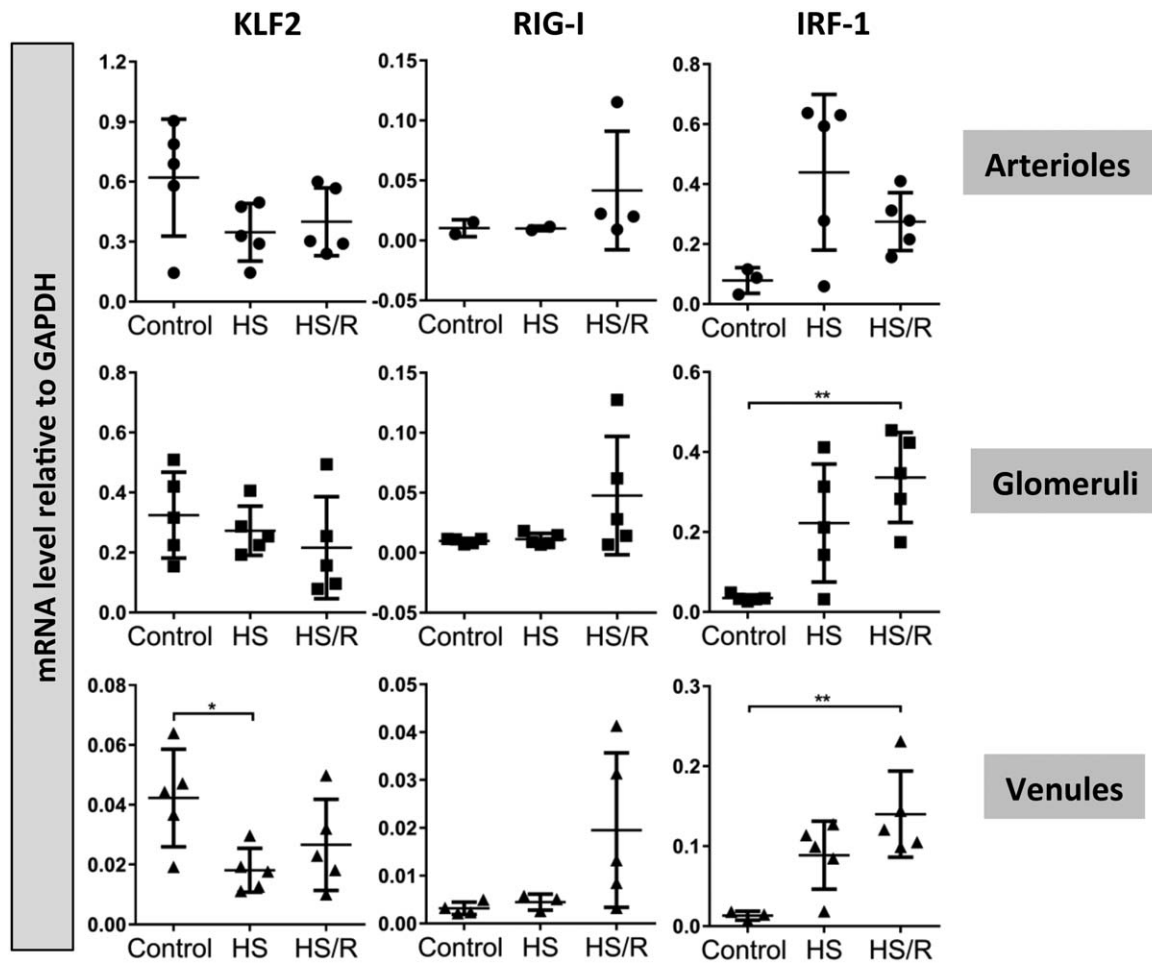
FIG. 4. **Expression of intracellular signaling molecules KLF2, RIG-I, and IRF-1 in renal microvascular compartments in healthy kidney and effects of HS and HS/R.** Gene expression levels of KLF2, RIG-I, and IRF-1 were assessed by RT-qPCR in arterioles, glomeruli, and venules obtained by laser microdissection from snap-frozen tissues of control mice, HS mice, and HS/R mice, using GAPDH as the reference gene. Individual values and mean $\pm$ SD are shown for each group. N.D., not detectable. $^*P < 0.05$; $^{**}P < 0.01$. Groups with less than three samples were excluded from the statistical analysis.

during resuscitation did not have obvious effects on the response to HS/R of any renal segment regarding vascular stability related molecules, except for the strong inhibition of VEGFR2 expression in postcapillary venules. In venules, approximately 30% of the HS/R-associated expression of VEGFR2 remained (Fig. 5A). With regard to endothelial adhesion molecules and proinflammatory cytokines, the NF-κB inhibitor affected different molecules to various extents, though the number of affected molecules and the extent of effects were limited. The blockade of NF-κB signaling markedly suppressed HS/R-associated E-selectin induction in venules, and ICAM-1 induction in glomeruli and venules. In contrast, P-selectin and IL-6 were upregulated in the glomerular segments upon BAY11-7082 treatment (Fig. 5B). NF-κB inhibition furthermore significantly increased KLF2 expression mainly in arterioles, whereas it inhibited HS/R-induced IRF-1 expression in all three segments (Fig. 5C). These results demonstrate that BAY11-7082 treatment limited endothelial proinflammatory activation, though to a minor extent and with different effects in different renal microvascular segments.

Protein expression of endothelial cell adhesion molecules in renal microvascular compartments during HS, resuscitation, and NF-κB inhibition

To validate the mRNA data regarding the endothelial responses to HS, HS/R, and BAY11-7082 treatment at protein level, we immunohistochemically (IHC) stained mouse kidneys and semiquantitatively assessed the staining. We focused on the same three microvascular segments as studied using laser microdissection/RT-qPCR. E-selectin protein was absent from all three microvascular segments in healthy control kidneys (IHC staining not shown). Resuscitation upregulated E-selectin expression most prominently in glomeruli and venules. In arterioles also a similar increase was observed, but the extent of upregulation was lower and statistically not significant. BAY11-7082 treatment did not have a distinct effect on E-selectin induction in the microvascular beds (Fig. 6). In control conditions, VCAM-1 protein was expressed mainly in arterioles and venules, but not in glomeruli (Supplementary Fig. S1B, http://links.lww.com/SHK/A710). One hour after resuscitation, VCAM-1 protein was visible in the glomerular segments, an increase
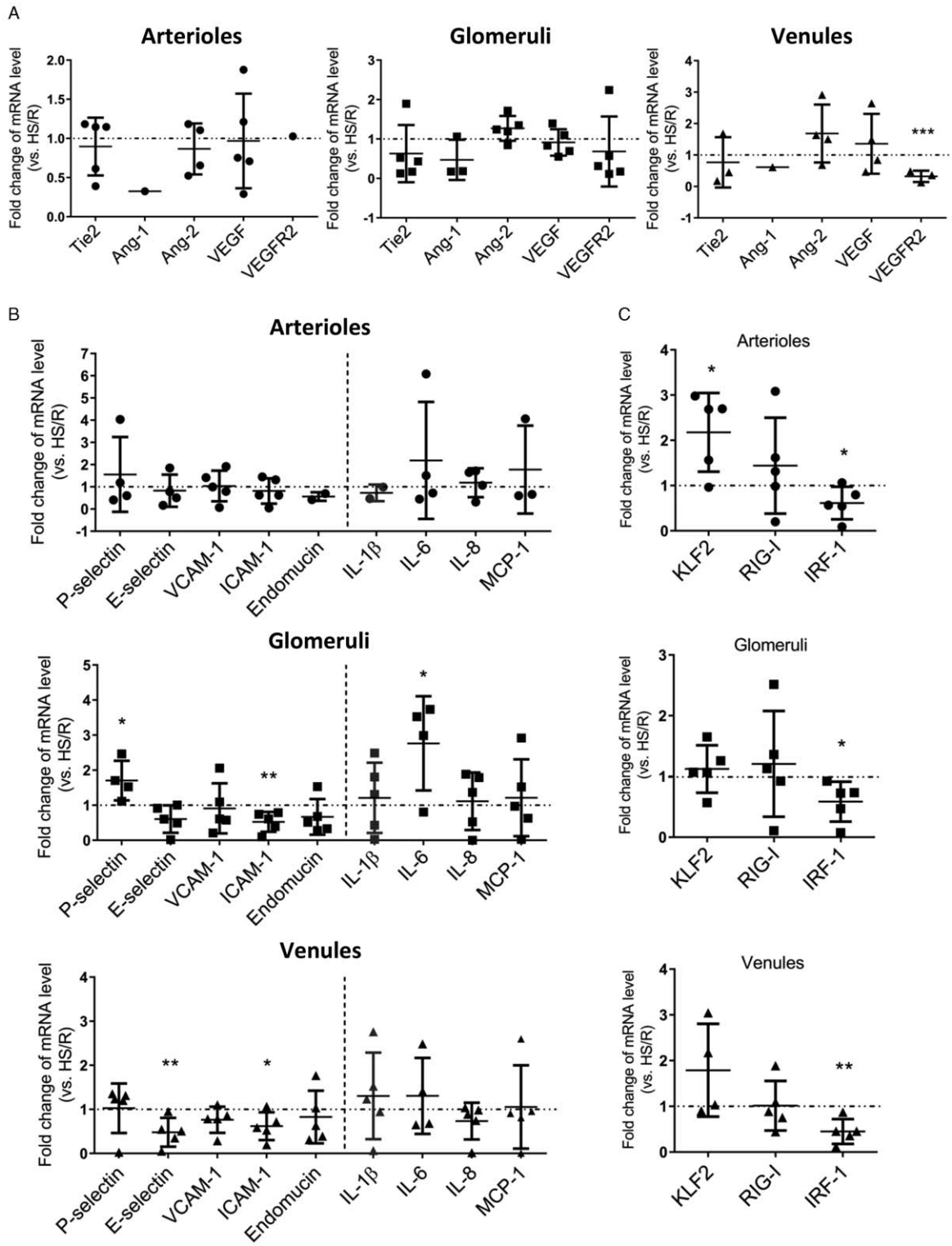
FIG. 5. **Effects of the NF-κB inhibitor BAY11-7082 administered during resuscitation on HS/R-induced endothelial proinflammatory activation in renal microvascular compartments.** mRNA expression of vascular stability related molecules (A), endothelial adhesion molecules and proinflammatory cytokines (B), and intracellular signaling molecules (C) was analyzed by RT-qPCR in the three renal microvascular segments of mice resuscitated with vehicle or treated with BAY11-7082 during resuscitation. VE-cadherin or GAPDH was used as reference gene. Values represent the fold change of the HS/R/BAY group relative to the HS/R group. Individual values and mean ± SD are shown for each group. N.D., not detectable. $^{*}P < 0.05$; $^{**}P < 0.01$. Groups with less than three samples were excluded from the statistical analysis.
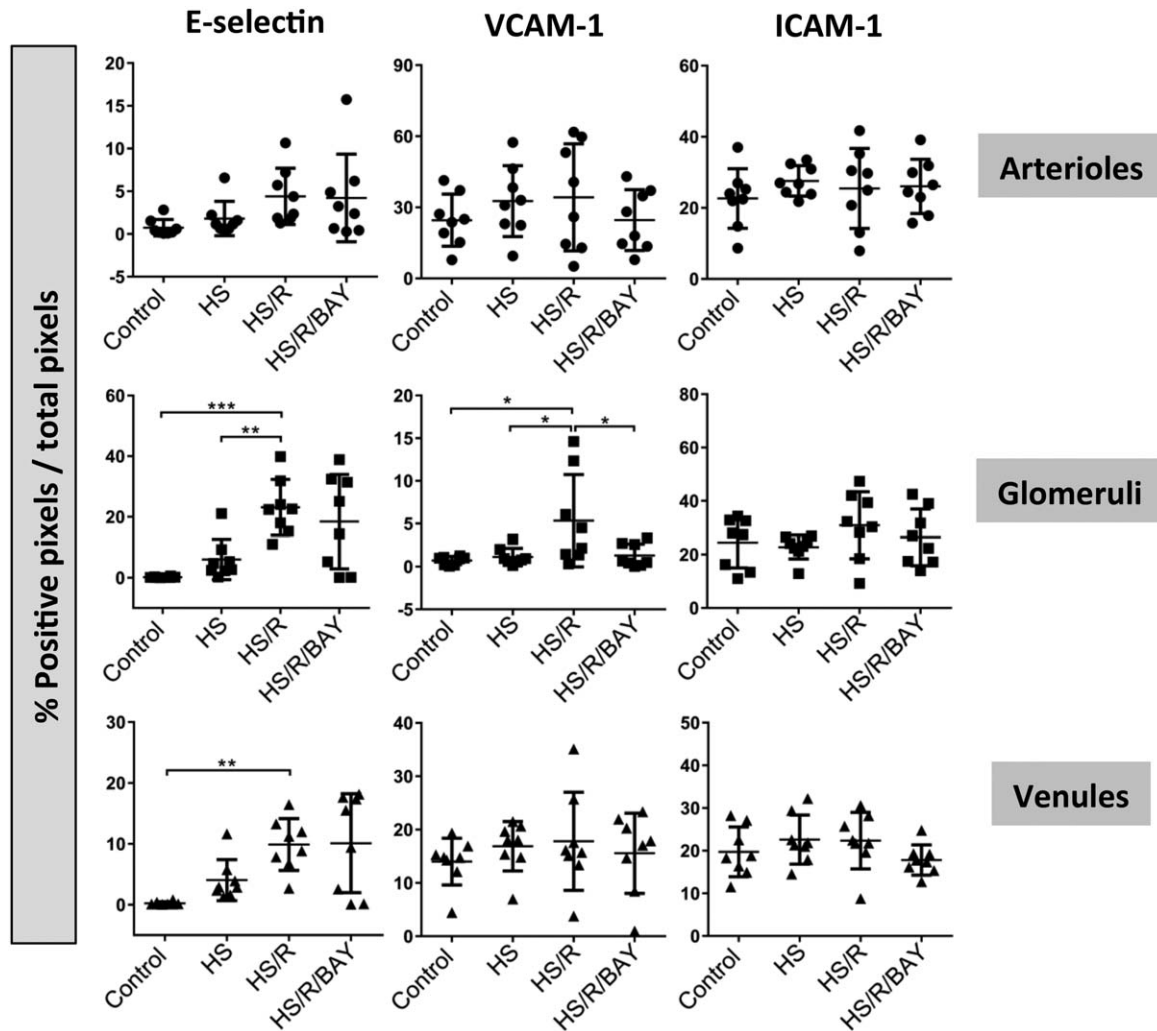
FIG. 6.   **Quantification of protein expression of endothelial cell adhesion molecules in renal microvascular compartments during HS, HS/R, and HS/ R/NF-κB inhibition.** Morphometric data obtained from immunohistochemical (IHC) staining of proteins E-selectin, VCAM-1, and ICAM-1 in kidney sections of mice subjected to HS followed by resuscitation in the absence or presence of BAY11-7082. The endothelial microvascular compartments of the kidney that were analyzed for semiquantitation are shown in Figure 1B. $^*P < 0.05$; $^{**}P < 0.01$; $^{***}P < 0.001$.

that was inhibited by BAY11-7082 treatment during resuscitation (Fig. 6). ICAM-1 protein was expressed to a similar level in all vascular segments in healthy kidneys, with no expression changes after HS and HS plus resuscitation (Supplementary Fig. S1B, http://links.lww.com/SHK/A710). Furthermore, BAY11-7082 treatment did not have an effect on ICAM-1 protein expression in the microvascular segments (Fig. 6).

Kinetics of NF-κB nuclear translocation in the glomeruli in mouse kidney to explain the limited effects of NF-κB inhibitor treatment during resuscitation

To investigate NF-κB activation kinetics and to what extent the NF-κB inhibitor affected the NF-κB signaling during HS/R, we stained mouse kidney sections using IF double staining for NF-κB subunit p65 and endothelial marker CD31. In glomerular endothelial cells, as shown in Figure 7, HS already resulted

in significant p65 nuclear translocation, which did not further increase during the resuscitation phase. Blockade of the NF-κB pathway by BAY11-7082 reduced p65 nuclear translocation, but did not fully inhibit this process during resuscitation (Fig. 7). These data thus indicate that already during the HS period NF-κB signaling was activated, and that BAY11-7082 treatment during the resuscitation phase could partly counteract this proinflammatory pathway.

DISCUSSION

HS causes both macrocirculatory and microcirculatory dysfunction. The persistence of microcirculatory impairment can result in multiple organ failure, and one of the prime target organs is the kidney (22). In the present study, we explored the responses of arterioles, glomeruli, and postcapillary venules to
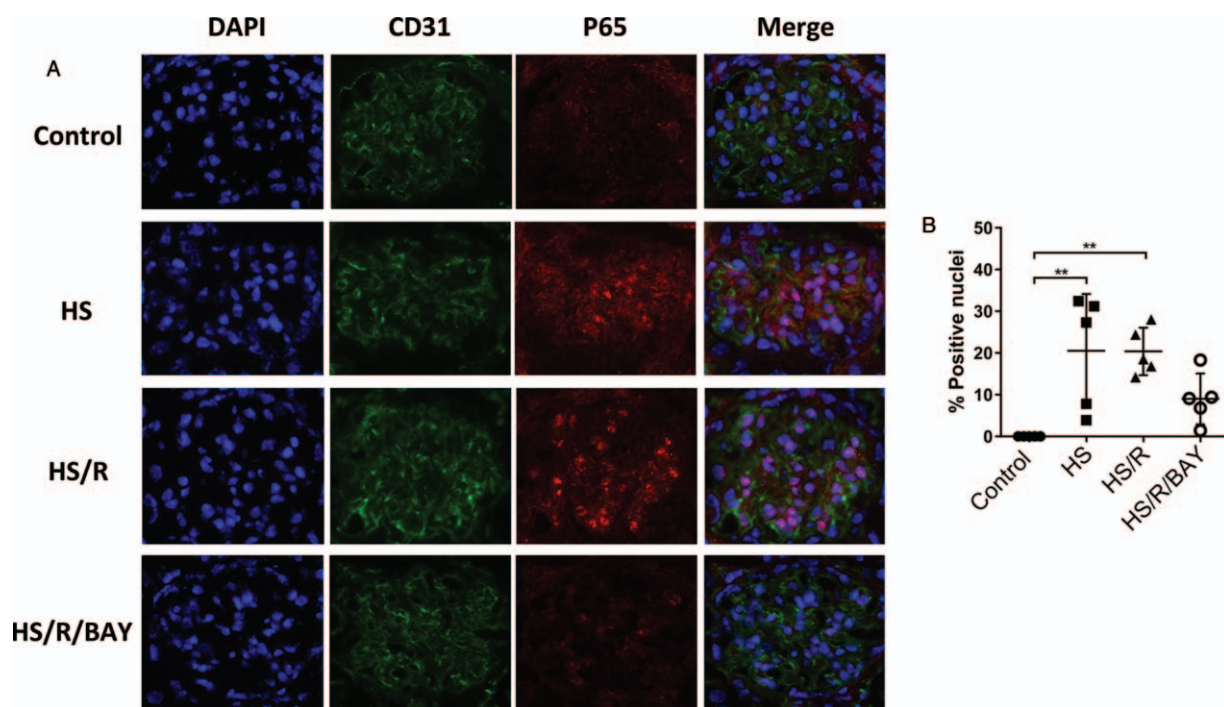
Fig. 7.   **Effects of the NF-κB inhibitor BAY11-7082 on HS/R-induced NF-κB nuclear translocation in glomeruli during resuscitation in mouse kidney.** (A) Immunofluorescence staining for the NF-κB subunit p65 (red), the endothelial marker CD31 (green), and nuclei (DAPI nuclear staining, blue) in the glomeruli of control mice, HS mice, HS/R mice, and HS/R mice treated with BAY11-7082 during resuscitation. All images were taken with equal exposure times. Original magnification 400×. Figures show representative images of each group. (B) Percentages of p65 positive nuclei were calculated: at least 10 glomeruli per mouse were analyzed and percentages were averaged. Individual average values and mean ± SD are shown for each group (n = 5). $^{**}P < 0.01$.

90 min HS and subsequent resuscitation (HS/R), and the effect of therapeutic intervention with NF-κB inhibitor BAY11-7082 during the resuscitation period on these responses. We found differential expression of the vascular integrity related molecules, with Tie2 and VEGFR2 being markedly decreased in glomeruli in response to HS and resuscitation, whereas the Ang-2 expression was significantly increased in this microvascular segment. Furthermore, HS/R strongly upregulated endothelial adhesion molecules, proinflammatory cytokines, and chemokines. Also, the intracellular signaling molecule IRF-1, which is involved in RIG-I controlled endothelial inflammatory responses (17, 21), was significantly upregulated. These responses mainly occurred in glomeruli and postcapillary venules. Nuclear translocation of NF-κB, reflecting cell activation via this signaling pathway, already occurred during the HS period, which is likely the main reason why pharmacological blockade of this pathway during the resuscitation period with BAY11-7082 had a minor effect on HS/R-induced microvascular endothelial cell activation. Taken together, our findings demonstrate that endothelial cells especially in glomeruli and postcapillary venules engage in the proinflammatory response during HS/R and respond to NF-κB inhibition, though the extent differed between these segments. The arteriolar segments were less responsive to HS/R, which is not surprising because their main function is to regulate vascular resistance and blood flow.

HS and resuscitation strongly upregulated E-selectin mRNA levels in glomeruli, which was paralleled by noticeably enhanced glomerular E-selectin protein expression. Furthermore, VCAM-1 and ICAM-1 mRNA levels were significantly upregulated after resuscitation in glomeruli and venules. However, semiquantitative analyses based on immunohistochemical detection did not confirm the induction of these two proteins. Possibly, this is due to high constitutive protein expression levels in healthy conditions in these segments that do not allow identification of further enhancement of expression. As in glomeruli VCAM-1 protein showed lower expression levels in healthy conditions, resuscitation-induced upregulation of this protein was visible and paralleled VCAM-1 mRNA induction in this microvascular bed. Moreover, the inhibitory effects of BAY11-7082 treatment on E-selectin mRNA expression could not be confirmed at the protein level. Possibly, the time interval needed for mRNA to be translated into protein was too short. Analyzing protein expression at later time points after resuscitation may possibly provide more evidence to confirm the mRNA expression of adhesion molecules.

Endomucin (EMCN) was mainly expressed in glomeruli and venules in healthy mouse kidney, which is in line with a previous report (23). A recent study in HUVEC showed that proinflammatory cytokine TNF-α downregulated EMCN mRNA and protein expression, concurrent with an increase in E-selectin, VCAM-1, and ICAM-1 expression. This study furthermore showed that EMCN prevented leukocyte contact with adhesion molecules, and that overexpression of EMCN reduced TNF-α-induced inflammatory cell infiltration in

mouse ciliary bodies (24). In the present study, HS followed by resuscitation markedly downregulated EMCN expression in glomeruli. This downregulation of EMCN may facilitate leukocyte-endothelial cell interaction and accelerate HS/R-induced proinflammatory status within the glomeruli. IHC staining for CD45 positive leukocytes showed that the number of adherent CD45 positive leukocytes was significantly increased after 90 min HS in glomeruli. However, we did not observe a further increase in numbers of CD45 positive cells after resuscitation (data not shown). Perhaps some of these leukocytes had transmigrated into the underlying tissue, or adherent leukocytes reentered the blood when the blood flow recovered during resuscitation. It will be interesting to analyze the protein levels of EMCN after HS/R in future studies, and also to determine whether EMCN is shed from the endothelial cell membrane in inflammation conditions.

The angiopoietin (Ang)-Tie2 system does not only play a critical role in regulating vascular integrity, but it is also actively involved in inflammatory responses (25). Ang-1 was shown to reduce plasma leakage in inflammation and to suppress endothelial inflammation (26, 27). In contrast, Ang-2 binding to Tie2 sensitizes endothelial cells to TNF-α to facilitate endothelial activation (28), and promotes vascular leakage (29). In our study, a distinct decrease in Tie2 mRNA level in arterioles and glomeruli, and in Ang-1 expression in whole kidney sections (detection in segments of Ang-1 was not feasible) due to HS/R, was observed. This together with a strong increase in Ang-2 mRNA level in glomeruli suggests that the balance within the Ang-Tie2 ligand-receptor system was disturbed after resuscitation. Sison et al. reported that VEGF-VEGFR2 signaling has a key regulatory role in the maintenance of endothelial cell integrity in the glomerular microvasculature (30). In our study, also VEGFR2 mRNA expression was markedly decreased in glomeruli in response to HS/R, which may be associated with the loss of glomerular filtration barrier function. Whether loss of endothelial integrity and plasma leakage occurs in the microvascular segments of the kidney, e.g., by assessing proteinuria and urine Ang-2 protein levels, is worth investigating in future HS/R experiments.

In the present study, we found in healthy mouse kidneys that KLF2 mRNA levels in arterioles and glomeruli were much higher than in venules. KLF2 is regulated in endothelial cells by shear stress (31). As the normal values of shear stress at the blood vessel walls range between 10 and 70 dynes/cm^2 for arteries and between 1 and 6 dynes/cm^2 for veins (32), it is not surprising that renal postcapillary venules had the lowest expression of KLF2. Ninety minutes of HS downregulated KLF2 expression most prominently in the venular segments, a corroborating previous work from our laboratory showing that loss of shear stress rapidly inhibited the expression of KLF2 (19). HS and resuscitation can be considered as a systemic ischemia and reperfusion injury insult with major disturbances in blood flow related shear stress changes. In addition, HS/R markedly induces proinflammatory cytokine TNF-α and IL-1β expression in mouse kidney (15), which can also inhibit KLF2 expression in endothelial cells (33). A previous article showed that TNF-α-mediated reduction in KLF2 expression was controlled via NF-κB and histone deacetylase pathways (34). Such

a control mechanism could explain the increase in KLF2 expression in arterioles resulting from pharmacological NF-κB inhibition as observed in our study. Why this would only be happening in arterioles and not other microvascular segments remains unclear at present.

In our study, the mice in the four groups were terminated at different time points to investigate heterogenic responses of the microvascular segments in the kidney in response to HS only and in response to HS plus resuscitation in the absence or presence of an NF-κB inhibitor. We cannot rule out that differences in gene expression between HS and HS/R groups are partly caused by the difference in time of sacrifice (90 min HS vs. 90 min plus resuscitation time 60 min HS/R), yet this experimental design allowed answering our research questions.

Immunofluorescence staining for NF-κB subunit p65 showed that in the glomeruli p65 nuclear translocation already occurred during HS conditions. This indicates that the NF-κB pathway was already activated during the HS period, which can explain why the blockade of NF-κB signaling during the resuscitation period only had a minor effect on proinflammatory activation of the renal microvasculature. From a clinical point of view, drug intervention aimed at inhibiting this pathway after a period of 90 min of HS will come too late. To be able to suppress the strong inflammatory response, drug intervention should be carried out at an earlier time point. In the surgical ward, severe bleeding can lead to HS, e.g., during large surgery. In contrast to HS induced by trauma, surgery patients could be treated with NF-κB inhibitors before or during surgery to prevent HS-induced endothelial inflammatory activation. Future studies should explore whether pretreatment with NF-κB inhibitors before HS or during surgery limits HS-mediated organ failure.

In the present study, a potential negative effect of NF-κB inhibitor treatment was revealed. Resuscitation with BAY11-7082 strongly inhibited VEGFR2 mRNA expression in venules. This can be explained by the fact that the VEGFR2 promoter contains an NF-κB-binding site, which is essential in mediating the expression of VEGFR2 (35). A similar observation was reported by Dong et al., who showed in HUVECs that dihydroartemisinin reduced VEGFR2 expression via inhibition of the NF-κB pathway (36).

In our study, we laser microdissected vascular compartments of the kidney. The advantage of using LMD is that it can precisely isolate-specific microvascular segments from renal tissue sections without affecting RNA integrity. Isolated segments retain their molecular status dictated by their *in vivo* microenvironment, thereby avoiding transcriptional changes as observed when culturing endothelial cells (37). As such, important new information on *in vivo* microvascular behavior can be revealed without the need for transgenic mouse models. The limitation is that LMD is a time-consuming technique. Furthermore, for genes expressed to a low extent, the square micrometer microvascular materials dissected did not always provide sufficient RNA for low-density array analysis. In this study, 19 different mRNA species were analyzed in 80 samples obtained from whole kidney sections and microvascular segment samples, with 238 out of 1,405 PCR reactions resulting in nondetectable signals that had to be excluded from the data analysis.

In summary, our findings show first of all that vascular stability related molecules and endothelial adhesion molecules are heterogeneously expressed in arterioles, glomeruli, and postcapillary venules in healthy mouse kidney. Furthermore, we provide evidence that endothelial cells in arterioles, glomeruli, and postcapillary venules become strongly activated by HS and resuscitation. The responses differed between microvascular segments, with strongest inflammatory responses mainly occurring in glomeruli and venules. In addition, NF-κB inhibitor BAY11-7082 treatment during the resuscitation phase ameliorated endothelial inflammatory responses to a minor extent, likely due to the fact that the NF-κB pathway already becomes activated early on in the HS phase. The here chosen study strategy may help to discover microvasculature-specific pathophysiological mechanisms of HS/R-induced renal dysfunction in the complex microenvironment in the kidney. The results can assist in choosing inhibitory drugs specifically aimed at an activation pathway in one particular segment once this pathway has been elucidated. Our research strategy furthermore assists in improving our pharmacological understanding of drug intervention outcomes aimed at particular renal microvascular segments. Although this has not been investigated in the present study, the application to new studies in mouse models and clinical samples may in the future provide valuable new insights that are crucial for design of clinical intervention strategies to prohibit renal dysfunction from happening.

ACKNOWLEDGMENTS

REFERENCES

1. Wang Y, Yan J, Xi L, Qian Z, Wang Z, Yang L: Protective effect of crocetin on hemorrhagic shock-induced acute renal failure in rats. *Shock* 38(1):63–67, 2012.

2. Kholmukhamedov A, Czerny C, Hu J, Schwartz J, Zhong Z, Lemasters JJ: Minocycline and doxycycline, but not tetracycline, mitigate liver and kidney injury after hemorrhagic shock/resuscitation. *Shock* 42(3):256–263, 2014.

3. Barrantes F, Tian J, Vazquez R, Amoateng-Adjepong Y, Manthous CA: Acute kidney injury criteria predict outcomes of critically ill patients. *Crit Care Med* 36(5):1397–1403, 2008.

4. Aird WC: Endothelial cell heterogeneity. *Cold Spring Harb Perspect Med* 2(1):a006429, 2012.

5. Aird WC: Phenotypic heterogeneity of the endothelium: II. Representative vascular beds. *Circ Res* 100(2):174–190, 2007.

6. Molema G, Aird WC: Vascular heterogeneity in the kidney. *Semin Nephrol* 32(2):145–155, 2012.

7. Molema G: Heterogeneity in endothelial responsiveness to cytokines, molecular causes, and pharmacological consequences. *Semin Thromb Hemost* 36(3):246–264, 2010.

8. van Meurs M, Wulfert FM, Knol AJ, De Haes A, Houwertjes M, Aarts LP, Molema G: Early organ-specific endothelial activation during hemorrhagic shock and resuscitation. *Shock* 29(2):291–299, 2008.

9. Asgeirsdottir SA, van Solingen C, Kurniati NF, Zwiers PJ, Heeringa P, van Meurs M, Satchell SC, Saleem MA, Mathieson PW, Banas B, et al.: MicroRNA-126 contributes to renal microvascular heterogeneity of VCAM-1 protein expression in acute inflammation. *Am J Physiol Renal Physiol* 302(12):F1630–F1639, 2012.

10. Liu SF, Malik AB: NF-kappa B activation as a pathological mechanism of septic shock and inflammation. *Am J Physiol Lung Cell Mol Physiol* 290(4):L622–L645, 2006.

11. Lawrence T: The nuclear factor NF-kappaB pathway in inflammation. *Cold Spring Harb Perspect Biol* 1(6):a001651, 2009.

12. Chima RS, Hake PW, Piraino G, Mangeshkar P, Denenberg A, Zingarelli B: Ciglitazone ameliorates lung inflammation by modulating the inhibitor kappaB protein kinase/nuclear factor-kappaB pathway after hemorrhagic shock. *Crit Care Med* 36(10):2849–2857, 2008.

13. Korff S, Loughran P, Cai C, Lee YS, Scott M, Billiar TR: Eritoran attenuates tissue damage and inflammation in hemorrhagic shock/trauma. *J Surg Res* 184(2):e17–e25, 2013.

14. Sordi R, Chiazza F, Johnson FL, Patel NS, Brohi K, Collino M, Thiemermann C: Inhibition of IkappaB kinase attenuates the organ injury and dysfunction associated with hemorrhagic shock. *Mol Med* 21:563–575, 2015.

15. Li R, Aslan A, Yan R, Jongman RM, Moser J, Zwiers PJ, Moorlag HE, Zijlstra JG, Molema G, van Meurs M: Histone deacetylase inhibition and IkappaB kinase/nuclear factor-kappaB blockade ameliorate microvascular proinflammatory responses associated with hemorrhagic shock/resuscitation in mice. *Crit Care Med* 43(12):e567–e580, 2015.

16. Langenkamp E, Kamps JA, Mrug M, Verpoorte E, Niyaz Y, Horvatovich P, Bischoff R, Struijker-Boudier H, Molema G: Innovations in studying in vivo cell behavior and pharmacology in complex tissues—microvascular endothelial cells in the spotlight. *Cell Tissue Res* 354(3):647–669, 2013.

17. Yan R, van Meurs M, Popa ER, Jongman RM, Zwiers PJ, Niemarkt AE, Kuiper T, Kamps JA, Heeringa P, Zijlstra JG, et al.: Endothelial interferon regulatory factor 1 regulates lipopolysaccharide-induced VCAM-1 expression independent of NFkappaB. *J Innate Immun* 9(6):546–560, 2017.

18. Kinoshita M, Nakamura T, Ihara M, Haraguchi T, Hiraoka Y, Tashiro K, Noda M: Identification of human endomucin-1 and -2 as membrane-bound O-sialoglycoproteins with anti-adhesive activity. *FEBS Lett* 499(1–2):121–126, 2001.

19. Li R, Zijlstra JG, Kamps JA, van Meurs M, Molema G: Abrupt reflow enhances cytokine-induced proinflammatory activation of endothelial cells during simulated shock and resuscitation. *Shock* 42(4):356–364, 2014.

20. DeVerse JS, Sandhu AS, Mendoza N, Edwards CM, Sun C, Simon SI, Passerini AG: Shear stress modulates VCAM-1 expression in response to TNF-alpha and dietary lipids via interferon regulatory factor-1 in cultured endothelium. *Am J Physiol Heart Circ Physiol* 305(8):H1149–H1157, 2013.

21. Moser J, Heeringa P, Jongman RM, Zwiers PJ, Niemarkt AE, Yan R, de Graaf IA, Li R, Ravasz Regan E, Kümpers P, et al.: Intracellular RIG-I signaling regulates TLR4-independent endothelial inflammatory responses to endotoxin. *J Immunol* 196(11):4681–4691, 2016.

22. Wu CY, Chan KC, Cheng YJ, Yeh YC, Chien CT: Effects of different types of fluid resuscitation for hemorrhagic shock on splanchnic organ microcirculation and renal reactive oxygen species formation. *Crit Care* 19:434, 2015.

23. Dimke H, Sparks MA, Thomson BR, Frische S, Coffman TM, Quaggin SE: Tubulovascular cross-talk by vascular endothelial growth factor a maintains peritubular microvasculature in kidney. *J Am Soc Nephrol* 26(5):1027–1038, 2015.

24. Zahr A, Alcaide P, Yang J, Jones A, Gregory M, dela Paz NG, Patel-Hett S, Nevers T, Koirala A, Luscinskas FW, et al.: Endomucin prevents leukocyte-endothelial cell adhesion and has a critical role under resting and inflammatory conditions. *Nat Commun* 7:10363, 2016.

25. Fiedler U, Augustin HG: Angiopoietins: a link between angiogenesis and inflammation. *Trends Immunol* 27(12):552–558, 2006.

26. Baffert F, Le T, Thurston G, McDonald DM: Angiopoietin-1 decreases plasma leakage by reducing number and size of endothelial gaps in venules. *Am J Physiol Heart Circ Physiol* 290(1):H107–H118, 2006.

27. Kim I, Moon SO, Park SK, Chae SW, Koh GY: Angiopoietin-1 reduces VEGF-stimulated leukocyte adhesion to endothelial cells by reducing ICAM-1, VCAM-1, and E-selectin expression. *Circ Res* 89(6):477–479, 2001.

28. Fiedler U, Reiss Y, Scharpfenecker M, Grunow V, Koidl S, Thurston G, Gale NW, Witzenrath M, Rosseau S, Suttorp N, et al.: Angiopoietin-2 sensitizes endothelial cells to TNF-alpha and has a crucial role in the induction of inflammation. *Nat Med* 12(2):235–239, 2006.

29. Milam KE, Parikh SM: The angiopoietin-Tie2 signaling axis in the vascular leakage of systemic inflammation. *Tissue Barriers* 3(1–2):e957508, 2015.

30. Sison K, Eremina V, Baelde H, Min W, Hirashima M, Fantus IG, Quaggin SE: Glomerular structure and function require paracrine, not autocrine, VEGF-VEGFR-2 signaling. *J Am Soc Nephrol* 21(10):1691–1701, 2010.

31. Dekker RJ, van Thienen JV, Rohlena J, de Jager SC, Elderkamp YW, Seppen J, de Vries CJ, Biessen EA, van Berkel TJ, Pannekoek H, et al.: Endothelial KLF2 links local arterial shear stress levels to the expression of vascular tone-regulating genes. *Am J Pathol* 167(2):609–618, 2005.

32. Papaioannou TG, Stefanadis C: Vascular wall shear stress: basic principles and methods. *Hellenic J Cardiol* 46(1):9–15, 2005.

33. SenBanerjee S, Lin Z, Atkins GB, Greif DM, Rao RM, Kumar A, Feinberg MW, Chen Z, Simon DI, Luscinskas FW, et al.: KLF2 is a novel transcriptional regulator of endothelial proinflammatory activation. *J Exp Med* 199(10):1305–1315, 2004.

34. Kumar A, Lin Z, SenBanerjee S, Jain MK: Tumor necrosis factor alpha-mediated reduction of KLF2 is due to inhibition of MEF2 by NF-kappaB and histone deacetylases. *Mol Cell Biol* 25(14):5893–5903, 2005.

35. Minami T, Rosenberg RD, Aird WC: Transforming growth factor-beta 1-mediated inhibition of the flk-1/KDR gene is mediated by a 5'-untranslated region palindromic GATA site. *J Biol Chem* 276(7):5395–5402, 2001.

36. Dong F, Zhou X, Li C, Yan S, Deng X, Cao Z, Li L, Tang B, Allen TD, Liu J: Dihydroartemisinin targets VEGFR2 via the NF-kappaB pathway in endothelial cells to inhibit angiogenesis. *Cancer Biol Ther* 15(11):1479–1488, 2014.

37. Calabria AR, Shusta EV: A genomic comparison of in vivo and in vitro brain microvascular endothelial cells. *J Cereb Blood Flow Metab* 28(1):135–148, 2008.